2012

Comparison of the removal of hydrophobic trace organic contaminants by forward osmosis and reverse osmosis

Ming Xie
University of Wollongong, mx504@uow.edu.au

Long D. Nghiem
University of Wollongong, longn@uow.edu.au

William E. Price
University of Wollongong, wprice@uow.edu.au

Menachem Elimelech
Yale University

Publication Details

Xie, M., Nghiem, L. D., Price, W. E. & Elimelech, M. (2012). Comparison of the removal of hydrophobic trace organic contaminants by forward osmosis and reverse osmosis. Water Research, 46 (8), 2683-2692.

Comparison of the removal of hydrophobic trace organic contaminants by forward osmosis and reverse osmosis

Water Research

Revised: February 2012

Ming Xie [1], Long D. Nghiem [1,*], William E. Price [2], and Menachem Elimelech [3]

[1] Strategic Water Infrastructure Laboratory, School of Civil Mining and Environmental Engineering, University of Wollongong, Wollongong, NSW 2522, Australia

[2] Strategic Water Infrastructure Laboratory, School of Chemistry, University of Wollongong, Wollongong, NSW 2522, Australia

[3] Department of Chemical Engineering, Environmental Engineering Program Yale University, New Haven, Connecticut 06520-8286, USA

---

* Corresponding author: Long Duc Nghiem, Email: longn@uow.edu.au; Ph +61 2 4221 4590

Abstract

We compared the rejection behaviours of three hydrophobic trace organic contaminants, bisphenol A, triclosan and diclofenac, in forward osmosis (FO) and reverse osmosis (RO). Using erythritol, xylose and glucose as inert reference organic solutes and the membrane pore transport model, the mean effective pore size of a commercial cellulose-based FO membrane was estimated to be 0.74 nm. When NaCl was used as the draw solute, at the same water permeate flux of 5.4 $L/m^2 \cdot h$ (1.5 μm/s), the adsorption of all three compounds to the membrane in the FO mode was consistently lower than that in the RO mode. Rejection of bisphenol A and diclofenac were higher in the FO mode compared to that in the RO mode. Because the molecular width of triclosan was larger than the estimated mean effective membrane pore size, triclosan was completely rejected by the membrane and negligent difference between the FO and RO modes could be observed. The difference in the separation behaviour of these hydrophobic trace organics in the FO (using NaCl the draw solute) and RO modes could be explained by the phenomenon of retarded forward diffusion of solutes. The reverse salt flux of NaCl hinders the pore diffusion and subsequent adsorption of the trace organic compounds within the membrane. The retarded forward diffusion effect was not observed when $MgSO_4$ and glucose were used as the draw solutes. The reverse flux of both $MgSO_4$ and glucose was negligible and thus both adsorption and rejection of BPA in the FO mode were identical to those in the RO mode.

Keywords: Forward osmosis, reverse osmosis, bisphenol A, triclosan, diclofenac, mean effective membrane pore size, retarded forward diffusion.

1. Introduction

Water scarcity is a major global challenge and is being further exacerbated due to continuing population growth, industrialization, contamination of available fresh water sources, and increasingly irregular weather patterns. Utilising unconventional water resources such as reclaimed wastewater has been identified as an important avenue for augmenting water supply and alleviating water stress (Shannon et al. 2008). Extraction of clean water from unconventional sources, including seawater and municipal wastewater, is arguably feasible from both technical and economic points of view (Elimelech and Phillip 2011, Shannon et al. 2008). However, the occurrence of trace organic contaminants in secondary treated effluent and sewage impacted water bodies in the range from a few nanogram per litre (ng/L) to several microgram per litre (μg/L), is a major obstacle for the implementation of water reuse (Basile et al. 2011, Carballa et al. 2004, Snyder et al. 2003). Although the full extent of the impact of these trace organic contaminants on human health is still a subject of intense scientific debate, some of these compounds have been shown to cause serious adverse effects on a range of organisms at environmentally relevant concentrations (Cunningham et al. 2009, Hansen et al. 1998, Rodgers-Gray et al. 2000). As a result, numerous investigations have been conducted to enhance the removal capacity of current treatment processes or develop new technologies for better removal of these trace organic contaminants from domestic wastewater and other impaired water resources (Shannon et al. 2008).

Forward osmosis (FO) has recently re-emerged as a potential technology that can improve the energy efficiency of water purification (Cath et al. 2006). In FO, clean water is extracted from a contaminated feed under an osmotic pressure gradient generated by the draw solution. Membrane fouling in the FO process has been shown to be less severe and more reversible than that with nanofiltration (NF) and reverse osmosis (RO) processes (Lee et al. 2010, Mi and Elimelech 2010, Ng and Elimelech 2004, Tang et al. 2010, Zou et al. 2011). Even when membrane fouling does occur, it is largely reversible and can be easily controlled by a simple physical cleaning technique such as increasing the shear force (cross flow velocity) at the membrane surface (Mi and Elimelech 2010). Consequently, there have been several successful demonstrations of FO for the treatment of wastewater with high fouling propensity with no or limited pretreatment, such as landfill leachate (Herron 1997), anaerobic digester concentrate (Holloway et al. 2007), activated sludge solution (Achilli et al. 2009, Cornelissen et al. 2008), and domestic wastewater (Cath et al. 2005, Valladares Linares et al. 2011).

Cath et al. (2010) proposed a novel hybrid system that combined the FO and RO processes for simultaneous water reuse and seawater desalination. In this hybrid system, domestic wastewater is first treated by an FO membrane and clean water is transported into a seawater draw solution. The diluted draw solution is subsequently desalinated by RO to produce clean water. This novel approach provides a double treatment barrier particularly for trace organic contaminants with a potentially lower energy footprint compared to current practice (Elimelech and Phillip 2011, Yangali-Quintanilla et al. 2011). Another system that combines FO and RO processes is the osmotic MBR (Achilli et al. 2009, Cornelissen et al. 2011). In this process, the wastewater passes through two semipermeable membranes in the FO processes and the RO process that used to separate and recycle the draw solution, thus providing a dual barrier for trace organic contaminants. Hence, it is of paramount importance to better understand the removal of trace organic contaminants in the FO process and compare the removal behaviour to that of RO.

The structure of the selective barrier of FO membranes is similar to that of RO membranes. However, the filtration behaviour of FO and NF/RO may not be the same because these processes operate in two distinctive filtration modes: one is osmotically driven while the other is hydraulic pressure driven. Significant differences in membrane fouling between FO and RO modes have been noticed. Lee et al. (2010) compared the fouling behaviours in FO and RO modes, and reported that the thickness and compactness of the fouling layers during FO and RO filtration were significantly different. Mi and Elimelech (2010) reported that the fouling layer formed in the FO process was loose and could be easily removed by increasing shear force. Therefore, it hypothesized herein that the solute mass transfer characteristics in FO and RO may not be the same, thereby influencing the separation behaviours of trace organic contaminants in FO and RO.

In this study, we compare the separation of hydrophobic trace organic contaminants by a commercially available FO membrane in the FO and RO modes at the same permeate flux. The mean effective pore size of the membrane was estimated to facilitate the understanding of separation behaviour using reference organic solutes and the steric hindrance pore transport model. Adsorption of the hydrophobic trace organic contaminants to the membrane was quantified and related to their rejection in the FO and RO modes. Solute mass transfer in the FO and RO modes was compared and delineated to elucidate the mechanisms governing the removal of trace organic contaminants in FO and RO modes.

2. Materials and methods

2.1. Forward osmosis membrane and membrane characterization

An asymmetric FO membrane acquired from Hydration Technologies Innovation (HTI, Albany, OR) was used in this investigation. The FO membrane, embedded in a polyester mesh for mechanical support, has a dense, moderately hydrophilic cellulose triacetate active layer. More details on the FO membrane are provided elsewhere (Cath et al. 2006, McCutcheon and Elimelech 2008).

Contact angle measurement was conducted by a Rame-Hart goniometer (Model 250, Rame-Hart, Netcong, NJ) using the standard sessile drop method. Room temperature was maintained at 21-22 °C during the measurement. An FO membrane coupon was submerged into Milli-Q water and shaken overnight before drying in a desiccator for contact angle measurement. Contact angles on both sides of the membrane were measured. At least ten droplets on each membrane sample were analysed.

2.2. Representative trace organic contaminants

Bisphenol A (endocrine disrupting compound), triclosan (antibacterial and antifungal agent), and diclofenac (non-steroidal anti-inflammatory drug) were selected as representative hydrophobic trace organic contaminants. These hydrophobic compounds are ubiquitous trace organic contaminants in secondary treated effluent and non-potable recycled water. They were selected primarily because of their suitable molecular dimensions and physicochemical properties to provide variable 'solute-membrane' interactions and subsequent removal behaviour. Their key physicochemical properties and molecular structures are presented in Table 1. The compounds were purchased from Sigma–Aldrich (St. Louis, MO) and their reported purity is 99% or higher. The trace organic contaminants were first dissolved in pure methanol to make up stock solutions of 2 g/L. The stock solutions were stored at -18 °C and were used within one month.

[Table 1]

2.3. Forward osmosis and reverse osmosis laboratory systems

FO experiments were conducted using a closed-loop bench-scale FO membrane system (Supplementary Data, Figure S1). The membrane cell was made of acrylic plastic and had channel dimensions of 13 cm long, 9.5 cm wide, and 0.2 cm deep. The total effective membrane area was 123.5 cm^2.

Two variable speed gear pumps (Micropump, Vancouver, WA) were used to circulate the feed and draw solutions. Flow rates of the feed and draw solutions were monitored using rotameters and kept constant at 1 L/min (corresponding to a cross flow velocity of 9 cm/s). The draw solution reservoir was placed on a digital balance (Mettler Toledo Inc., Hightstown, NJ) and weight changes were recorded by a computer to calculate the permeate water flux. The conductivity of the draw solution was continuously measured using a conductivity probe with a cell constant of 1 cm^{-1} (Cole-Parmer, Vernon Hills, Illinois). To maintain constant draw solution concentration, a peristaltic pump was regulated by a conductivity controller to intermittently dose a small volume of a concentrated draw solution (6 M of NaCl or 4 M $MgSO_4$ depending on the draw solution type) into the draw solution reservoir (control accuracy was ± 0.1 mS/cm). The concentrated draw solution makeup reservoir was also placed on the same digital balance. This setup ensured that the transfer of liquid between the two reservoirs did not interfere with the measurement of permeate water flux and that the system could be operated at a constant osmotic pressure driving force during the experiment. Manual control of draw solution concentration was applied when neutral glucose was used as draw solute in the FO experiment. A concentrated glucose (6 M) was manually added into the draw solution reservoir every two hours to minimize the dilution of the draw solution and the decline of osmotic pressure driving force.

A laboratory-scale cross-flow RO system with a rectangular stainless-steel crossflow cell was used in this study (Supplementary Data, Figure S2). The cell had an effective membrane area of 40 cm^2 (4 cm × 10 cm) with a channel height of 0.2 cm. The unit was equipped with a Hydra-Cell pump (Wanner Engineering Inc., Minneapolis, MN). The temperature of the feed solution was kept constant using a chiller/heater (Neslab RTE 7) equipped with a stainless steel heat exchanger coil, which was submerged into a stainless steel reservoir. Permeate flow was measured by a digital flow meter (Optiflow 1000, Agilent Technologies, Palo Alto, CA) connected to a PC, and the cross flow rate was monitored using a rotameter.

2.4. Characterisation of membrane pore size

Three reference organic solutes, namely erythritol, xylose, and glucose (Sigma-Aldrich, Saint Louis, MO), were employed to estimate the mean effective pore size of the membrane. A feed solution containing 40 mg/L (as total organic carbon, TOC) of each organic solute in Milli-Q water was used. The membrane was pre-compacted at 18 bar for 1 hour in the RO system, and experiments were conducted at pressure of 8, 10, 12, 14, and 16 bar at a constant

crossflow velocity of 25 cm/s. After adjusting the pressure, the crossflow RO filtration system was run for 1 hour before taking permeate and feed samples for analysis.

We used the pore transport model that incorporates steric (size) exclusion and hindered convection and diffusion to estimate the membrane pore size from the rejection data of the reference organic solutes (López-Muñoz et al. 2009, Nghiem et al. 2004, Tsuru et al. 1995). In this model, the ratio of solute radius (r_s) to the membrane pore radius (r_p), $\lambda = r_s/r_p$, is linked by the distribution coefficient φ when only steric interactions are considered:

$$\varphi = (1-\lambda)^2 \quad (1)$$

The real rejection of the reference organic solutes (R_r) is determined from:

$$R_r = 1 - \frac{c_L}{c_o} = 1 - \frac{\varphi K_c}{1 - exp(-Pe)(1-\varphi K_c)} \quad (2)$$

where c_o and c_L are the solute concentration just outside the pore entrance and pore exit, respectively; Pe is the membrane Peclet number; φ is the distribution coefficient for hard-sphere particles when only steric interactions are considered; and K_c is the hydrodynamic hindrance coefficient. Details on the calculation of Pe and K_c are given elsewhere (Bungay and Brenner 1973, Nghiem et al. 2004).

The real rejection in Equation (2) relates to the solute permeate concentration at the membrane surface, which is different from the bulk concentration due to concentration polarization. We applied film theory to account for concentration polarization, and relate the observed rejection R_o to the real rejection by:

$$ln\frac{(1-R_r)}{R_r} = ln\frac{(1-R_o)}{R_o} - \frac{J_v}{k_f} \quad (3)$$

where k_f is the mass transfer coefficient, and J_v is the volumetric permeate flux.

The mass transfer coefficient (k_f) was experimentally determined using the method described by Sutzkover et al. (2000). Experiments were first conducted at a crossflow velocity of 25 cm/s by measuring the pure water flux, followed by adding NaCl into the feed reservoir to make up a feed salt concentration of 2000 mg/L, and measuring the permeate water flux and permeate salt concentration. This protocol was carried out at two different applied pressures of 10 and 16 bar. Knowing the permeate and feed salt concentrations (and thus, the corresponding osmotic pressures based on van't Hoff equation, π_p and π_b, respectively), the applied pressure (ΔP), the pure water flux (J_w), and the permeate flux with

194 the 2000 mg/L NaCl solution (J_{salt}) enables the evaluation of the salt concentration at the
195 membrane surface. This membrane surface concentration is used in the film model for
196 concentration polarization to determine the mass transfer coefficient (Sutzkover et al. 2000):

197 $$k_f = \frac{J_{salt}}{ln\left[\frac{\Delta P}{\pi_b - \pi_p}\left(1 - \frac{J_{salt}}{J_w}\right)\right]} \quad (4)$$

198 To estimate the membrane pore size, the following optimization process was applied. First,
199 the parameters φK_c and Pe/J_v that are uniquely related to R_r, were determined by fitting the
200 reference organic solute rejection data to the model (Equation 2) using an optimization
201 procedure (Solver, Microsoft® Excel). The parameters φK_c and Pe/J_v are a function of solely
202 the variable λ (ratio of solute radius to membrane pore radius, r_s/r_p) and thus were used to
203 obtain λ for each organic solute and the membrane. With the determined value of λ and the
204 given solute radius r_s, the membrane average pore radius was readily calculated for each
205 reference organic solute rejection data.

206 ## *2.5. Trace organic contaminant rejection experiments*

207 Bisphenol A, triclosan, or diclofenac were spiked into a background electrolyte solution (20
208 mM NaCl and 1 mM $NaHCO_3$) to obtain a feed solution concentration of 500 µg/L of one
209 specific trace organic contaminant. Either HCl (1 M) or NaOH (1 M) was introduced into the
210 feed tank to adjust the initial pH value of the feed solution to pH 7. Analytical grade NaCl,
211 $MgSO_4$, and glucose (Fisher Scientific, Pittsburgh, PA) were used to prepare the draw
212 solutions in Milli-Q water.

213 For the FO experiments, the initial volumes of the feed and draw solutions were 4 L and 1
214 L, respectively. The draw solutions used for the various experiments were 0.5 M NaCl, 3 M
215 glucose, or 2.5 M $MgSO_4$. Temperatures of the feed and draw solutions were kept constant at
216 25±1 °C using a temperature control unit (Thermo Fisher Scientific, Waltham, MA). A new
217 FO membrane coupon was used for each experiment. Approximately 1 mL of samples from
218 both the feed and draw solutions were taken at specific time intervals for HPLC analysis.

219 For the RO experiments, the initial volume of the feed solution was 4 L. The temperature
220 of the feed solution was kept constant at 25±1 °C using a chiller/heater (Neslab RTE 7). The
221 membrane was pre-compacted at 18 bar with deionised water for one hour prior to trace
222 organic contaminant rejection experiments. To simulate a similar flux pattern as that in the
223 FO mode, the permeate in the RO mode was not recirculated into the feed reservoir.

Experiments were conducted at a constant permeate flux (corresponding to an operating pressure of 10 bar) and at a constant crossflow velocity of 25 cm/s.

The rejection of trace organic contaminants in the RO is defined as

$$R_{RO} = (1 - \frac{C_{p(t)}}{C_{f(t)}})100\% \quad (5)$$

where, $C_{p(t)}$ and $C_{f(t)}$ are the concentration of target solute in the permeate and feed solution at time t, respectively. Unlike the RO process, the permeate concentration in the FO process is diluted by the draw solution. Hence, the actual (corrected) concentration of the target solute, $C_{s(t)}$, can be obtained by taking into account the dilution using a mass balance:

$$C_{s(t)} = \frac{C_{ds(t)}V_{ds(t)} - C_{ds(t-1)}V_{ds(t-1)}}{V_{w(t)}} \quad (6)$$

Here, $V_{w(t)}$ is the permeate volume of water to the draw solution at time t, $V_{ds(t-1)}$ is the volume of draw solution at time (t-1), $V_{ds(t)}$ is the volume of draw solution at time t, $C_{ds(t)}$ is the measured concentration of target solute in the draw solution at time t, and $C_{ds(t-1)}$ is the measured concentration of target solute in the draw solution at time (t-1). Subsequently, the solute rejection is calculated using the actual permeate concentration, yielding:

$$R_{FO} = (1 - \frac{C_{s(t)}}{C_{f(t)}})100\% \quad (7)$$

where $C_{f(t)}$ is the concentration of the target solute in the feed solution at t time.

The amount of trace organic contaminant adsorbed to the membrane was experimentally determined using an extraction procedure. At the completion of each FO or RO experiment, the membrane was removed from the membrane cell. Excess liquid on the membrane surface was allowed to drain off by gently tilting the membrane coupon. A predetermined size of membrane coupon (2.5 cm × 3 cm) was submerged in 10 mL of pure methanol in a sealed conical flask, which was placed on a shaker at a speed of 120 rpm at 20 °C for 12 hours. Aliquot sample of approximately 1 mL was taken at the end of the extraction procedure for HPLC analysis to quantify the amount of trace organic contaminant adsorbed onto the membrane. The amount of trace organic contaminant absorbed to the membrane was also determined by a mass balance calculation.

The reverse flux of draw solute in FO mode was determined using mass balance calculation:

$$J_{salt} = \frac{\left(C_t V_t - C_0 V_0\right)}{At} \quad (8)$$

where C_0 and C_t are the concentration of the draw solute in the feed at time 0 and t, respectively; V_0 and V_t are the volume of the feed at time 0 and t, respectively; A is the membrane area, and t is the operating time of the FO experiment. Draw solute concentrations of NaCl and $MgSO_4$ in the feed solution were determined using electric conductivity measurement based on the calibration curves of NaCl and $MgSO_4$, and that of glucose was determined using TOC measurement.

2.6. Analytical methods

A Shimadzu TOC analyser (TOC-V_{CSH}) was used to analyze the permeate concentration of the reference organic solutes. Concentration of glucose in the feed solution was also measured for the calculation of the reverse draw solute flux using the same TOC analyser. For trace organic contaminants rejection experiments, a Shimadzu HPLC system (Shimadzu, Kyoto, Japan) equipped with a Supelco Drug Discovery C-18 column (with diameter, length, and pore size of 4.6 mm, 150 mm, and 5 µm, respectively) and a UV–Vis detector was used to measure the concentrations of the trace organic contaminants in the feed and permeate (or draw solution) samples. A detection wavelength of 280 nm was employed. The mobile phase used for gradient elution was Milli-Q water buffered with 25 mM KH_2PO_4 and acetonitrile, and was delivered at 1 mL/min through the column. Calibration generally yielded standard curves with coefficients of determination (R^2) greater than 0.99 within the range of experimental concentrations used. The analysis was carried out immediately upon the conclusion of each experiment. A sample injection volume of 50 µL was used considering the salt tolerance of the C18 column. The quantification limit for all the analytes under investigation using these conditions was approximately 10 µg/L.

3. Results and discussion

3.1. Membrane pore size

Real rejection (R_r) of the reference organic solutes by the membrane at different permeate fluxes (Supplementary Data, Figure S3) was obtained from observed rejection (R_o) by accounting for concentration polarization (Equation 3). The real rejections data of the reference organic solutes were used to estimate the mean effective membrane pore size using the membrane pore transport model (Equation 2). The mean effective membrane pore radius

282 was determined to be 0.37 nm (equivalent to the mean effective membrane pore size of 0.74
283 nm) based on the obtained λ and molecular radii of three reference organic solutes (Table 2).

284 The pore size of the membrane is comparable to that of a "tight" nanofiltration membrane
285 such as the NF 90. Using the same membrane pore transport model, the average pore radius
286 of the NF 90 was determined to be 0.34 and 0.38 nm by Nghiem et al. (2004) and López-
287 Muñoz et al. (2009), respectively. In comparison, the membrane has a considerably smaller
288 pore radius than "loose" NF membranes, such as the NF 270 with a pore radius of 0.42 – 0.44
289 nm (López-Muñoz et al. 2009, Nghiem et al. 2004) and the BQ01 with a pore radius of 0.80
290 nm (Seidel et al. 2001). Based on the pore transport model, rejection of trace organic
291 contaminants by the HTI FO membrane is expected to be higher than that of a typical NF
292 membrane.

293 It is noteworthy that the active layer of the HTI FO membrane is made of cellulose
294 triacetate whereas the skin layer of most commercially available NF and RO membranes is
295 made of polyamide or its derivatives. Therefore, the intrinsic separation property of the FO
296 membrane may differ from that of a typical NF membrane. In fact, the HTI FO membrane
297 has a much lower permeability and a slightly higher NaCl rejection in comparison to most NF
298 membranes (Gray et al. 2006, Lee et al. 2010, Mi and Elimelech 2008). The measured pure
299 water permeability and NaCl rejection of the HTI FO membrane measured in the RO mode
300 were 1.1 L/ (m^2·h·bar) and 92.8 %, respectively. In comparison, it was reported that the pure
301 water permeability and NaCl rejection of the NF90 (which is known to be a tight NF
302 membrane) were 6.4 L/ (m^2·h·bar) and 85%, respectively (Nghiem et al. 2008).

303 The estimated mean effective membrane pore size allows for a systematic investigation of
304 the transport behaviours of the three selected hydrophobic trace organic contaminants. It is
305 noted that the molecular width of both bisphenol A and diclofenac (Table 1) is smaller than
306 the membrane pore size, while that of triclosan (Table 1) is larger than the membrane pore
307 size. In the following section, we explored the different removal behaviours of these
308 hydrophobic compounds in the FO and RO modes.

309 **[Table 2]**

3.2. Removal behaviour of hydrophobic trace organics in FO and RO modes

3.2.1 Bisphenol A

Bisphenol A is a hydrophobic compound with a distribution coefficient (log *D*) value of 3.64 (at experimental pH of 7) (Table 1). The measured contact angle of the HTI FO membrane in this study was 62.8±3.9°, which is similar to the value of 60.2±3.4° previously reported by McCutcheon and Elimelech (2008), indicating that the membrane is also moderately hydrophobic. Adsorption of bisphenol A to the membrane was observed in both the FO and RO modes as evident by the decrease in the feed concentration of the compound as the filtration process progressed (Figure 1). In fact, adsorption of hydrophobic trace organics to NF/RO membranes has been widely reported in the literature (Braeken et al. 2005, Schäfer et al. 2011).

When NaCl was used as the draw solution, there was a remarkable difference in the filtration behaviour of bisphenol A in the FO and RO modes (Figure 1). Even though the adsorption of bisphenol A to the membrane occurred in both the FO and RO modes, the adsorption process reached a quasi equilibrium state faster in the FO mode compared to the RO mode. In the FO mode, the feed concentration of bisphenol A decreased from 500 to 470 µg/L within the first 100 minutes. The small increase in the feed concentration of bisphenol A after 100 minutes of filtration can be explained by the continuous reduction in volume of the feed solution as water permeated through the membrane to the draw solution. In contrast, in the RO mode, it took almost 200 minutes for the feed concentration of bisphenol A to reach a stable value of approximately 420 µg/L. Both mass balance calculation and extraction measurement consistently showed that the amount of bisphenol A adsorbed to the membrane in the RO mode was significantly higher than that in the FO mode (Table 3).

It is notable that the rejection of bisphenol A in the FO mode was higher than that in the RO mode at the same permeate water flux (Figure 1). The bisphenol A rejection in the FO mode was comparable to the value previously reported by Hancock et al (2011) who examined the rejection of bisphenol A by the same membrane using similar concentration and type of draw solution, feed solution and experimental set-up. The rejection of bisphenol A in FO mode (Figure 1) was higher than that reported by Valladares Linares et al (2011). However, it is noted that unlike our study and that by Hancock et al (2011), in the study by Valladares Linares et al (2011), the FO membrane cell was submerged in the feed solution similar to a dead-end filtration configuration.

342 Rejection value of bisphenol A in the RO mode also agreed well with the estimated pore
343 radius of the membrane, whose pore size is larger than that of the NF270 membrane and
344 slightly smaller than that of the NF90 membrane. The rejection obtained by the membrane in
345 the RO mode was 75%. In comparison, bisphenol A rejection by the NF270 and NF90
346 membrane in the RO mode was 30 and 90%, respectively (Nghiem et al. 2008).

347 The higher rejection of bisphenol A in the FO mode compared to the RO mode when
348 operated at the same permeate water flux can be explained by the higher adsorption of this
349 compound to the membrane in the RO mode (Table 3). It has been previously established that
350 the adsorption of hydrophobic trace organic contaminants to the membrane can subsequently
351 facilitate their transport by diffusion through the membrane polymeric matrix (Nghiem et al.
352 2004). The molecular size of bisphenol A is slightly smaller than the mean effective
353 membrane pore size (Tables 1 and 2) and diffusive transport of this compound through the
354 membrane polymeric matrix is expected to be significant.

355 **[Figure 1]**

356 **[Table 3]**

357 ### *3.2.2 Triclosan*

358 Significant adsorption of triclosan, which has a log *D* value of 5.28 at pH 7 (Table 1), to the
359 membrane was also observed. The feed concentration of triclosan decreased significantly as
360 the filtration experiments progressed in both the FO and RO modes (Figure 2). In good
361 agreement with the results reported above for bisphenol A, the adsorption of triclosan to the
362 membrane reached a quasi equilibrium state faster in the FO mode than in the RO mode as
363 seen from the triclosan feed concentration profiles. It is also notable that the amount of
364 triclosan adsorbed to the membrane in the RO mode was significantly higher than that in the
365 FO mode (Table 4). However, because the molecular width of triclosan (0.75 nm) was larger
366 than the estimated mean effective pore size of the membrane (0.74 nm), a near complete
367 rejection of this compound was observed in both the FO and RO modes (Figure 2). In a
368 previous study, Hancock et al (2011) reported complete rejection of triclosan by the same
369 membrane. Similarly, near complete rejection of triclosan by the NF270 membrane which is
370 a loose NF membrane has also been reported by Nghiem and Coleman (2008).

371 **[Figure 2]**

372 **[Table 4]**

3.2.3 Diclofenac

Adsorption of diclofenac to the membrane (Table 5) was much smaller than bisphenol A and triclosan consistent with its low Log *D* value (1.77 at pH 7, Table 1). Because the feed volume continuously decreased in the FO mode, the feed concentration of diclofenac gradually increased as a function of time (Figure 3). In the RO mode, the adsorption of diclofenac to the membrane was higher than that in the FO mode (Table 5), which explains only slight increase in its feed concentration. It is also notable that diclofenac rejection was almost complete in the FO mode and was only approximately 90 % in the RO mode (Figure 3). The high rejection of diclofenac in both RO and FO modes is expected given its molecular dimension. It is noteworthy that although diclofenac has a similar molecular weight compared to triclosan, the shape of this compound is cylindrical (molecular modelling). The molecular width of diclofenac is slightly smaller than the estimated mean effective pore size of the membrane (Table 1). Consequently, it was possible to observe the difference in the rejection of diclofenac between the FO and RO modes at the same permeate flux (Figure 3).

[Figure 3]

[Table 5]

3.3. Reverse draw solute permeation retards the forward transport of hydrophobic organics

The marked difference in the separation behaviour of hydrophobic trace organics in the FO and RO modes discussed above could be attributed to their steric hindrance by the draw solute permeating through the membrane in the opposite direction. In the RO process, water permeates through the membrane under a hydraulic pressure gradient across the membrane and mass transfer can only occur in one direction from the feed side towards the permeate side of the membrane. In the FO process, water permeates from the feed solution to the draw solution under an osmotic pressure gradient generated by the concentrated draw solution across the membrane. As a result, the transport of water through the membrane in FO is coupled with the transport of the draw solute in the opposite direction (Figure 4).

[Figure 4]

The reverse NaCl flux in the FO experiments was significant (Table 6). We also note that the hydrated radii of Na^+ (0.36 nm) and Cl^- (0.33 nm) (Israelachvili 2010) were comparable to that of the membrane pore radius as well as the molecular dimensions of hydrophobic

404 organic contaminants investigated in this study. Thus, the reverse salt flux could hinder the
405 pore forward diffusion of the trace organic solute, leading to a lower adsorption of
406 hydrophobic trace organic within the membrane and subsequently higher rejection in the FO
407 mode than that in the RO mode.

408 **[Table 6]**

409 Our results are consistent with the "retarded forward diffusion" phenomenon suggested by
410 Hancock and Cath (2009) who examined the coupled diffusion of solutes in osmotically
411 driven membrane processes. They reported that the permeation of dissolved silica (SiO_2)
412 from the feed to the draw solution was lower when NH_4HCO_3 was used as the draw solute
413 instead of NaCl or $MgCl_2$. Hancock and Cath (2009) explained their observation by the
414 higher reverse flux of NH_4HCO_3 compared to that of both NaCl and $MgCl_2$ at the same
415 osmotic pressure of the draw solution. The results reported in this study and those observed
416 by Hancock and Cath suggest that the "retarded forward diffusion" phenomenon can be more
417 profound for hydrophobic trace organic contaminants because of their much lower
418 concentration in the feed solution and their ability to transport through the membrane via the
419 sorption-diffusion mechanism.

420 When the reverse draw solute flux is negligible, one would expect that the retarded
421 forward diffusion phenomenon would diminish. To verify this hypothesis, the adsorption and
422 rejection of BPA were examined at the same permeate water flux as that in the RO mode (i.e.,
423 5.4 $L/m^2 \cdot h$ (1.5 μm/s)) using glucose and $MgSO_4$ as the draw solutes. Glucose has a low
424 diffusion coefficient (6.9×10^{-10} m^2/s) and a Stokes radius of 0.32 nm which is comparable to
425 the membrane mean effective pore radius. $MgSO_4$ has a considerably low diffusion
426 coefficient (3.5×10^{-10} m^2/s) and the hydration radii of Mg^{2+} (0.43 nm) and SO_4^{2-} (0.40 nm)
427 (Israelachvili 2010) are larger than the membrane pore size. As a result, the reverse flux of
428 both glucose and $MgSO_4$ was negligible (Table 6). In the absence of substantial reverse flux
429 of the draw solute, the pore transport and the adsorption of BPA to the membrane in both FO
430 and RO modes were almost identical (Table 6). The rejections of BPA using glucose (77 %)
431 and $MgSO_4$ (76 %) as the draw solutes in the FO mode (Figure 5) were comparable to that in
432 the RO mode (76 %).

433 **[Figure 5]**

4. Conclusion

Rejection of three hydrophobic trace organic contaminants, namely bisphenol A, triclosan, and diclofenac, by a commercially available FO membrane was investigated in both the FO and RO modes. The separation behaviour of the trace organic compounds in the FO mode, when NaCl was used as the draw solute, differed from that in the RO mode. At the same water permeate flux of 5.4 L/m^2·h (or1.5 μm/s), adsorption of all three compounds to the membrane in the FO mode was consistently lower than that in the RO mode. In addition, the rejections of bisphenol A and diclofenac were higher in the FO mode compared to the RO mode. Because the molecular width of triclosan were larger than the estimated mean effective membrane pore size, the rejection of triclosan by the membrane was close to 100 % and negligible difference between the FO and RO modes could be observed. The difference in the separation behaviour of these hydrophobic trace organics in the FO (when NaCl was used as the draw solute) and RO modes could be explained by the retarded forward diffusion of feed solutes within the membrane pore. The relatively high reverse NaCl flux hinders the adsorption and diffusion of these trace organic compounds within the membrane pore matrix. The retarded forward diffusion phenomenon was verified by conducting experiments using draw solutions with much lower reverse salt flux, namely $MgSO_4$ and glucose. With these draw solutes, the adsorption and rejection of BPA in the FO mode were identical to that those in the RO mode.

5. Acknowledgment

We acknowledge the international postgraduate research scholarship (IPRS) provided by the Australian government and the university postgraduate award (UPA) provided by the University of Wollongong to Ming Xie to support his PhD study. Hydration Technology Innovations is thanked for the provision of the membrane samples.

6. References

Achilli, A., Cath, T.Y., Marchand, E.A. and Childress, A.E. (2009) The forward osmosis membrane bioreactor: A low fouling alternative to MBR processes. Desalination 239(1-3), 10-21.

Basile, T., Petrella, A., Petrella, M., Boghetich, G., Petruzzelli, V., Colasuonno, S. and Petruzzelli, D. (2011) Review of Endocrine-Disrupting-Compound Removal Technologies in Water and Wastewater Treatment Plants: An EU Perspective. Industrial & Engineering Chemistry Research 50(14), 8389-8401.

Braeken, L., Ramaekers, R., Zhang, Y., Maes, G., Bruggen, B.V.d. and Vandecasteele, C. (2005) Influence of hydrophobicity on retention in nanofiltration of aqueous solutions containing organic compounds. Journal of Membrane Science 252(1-2), 195-203.

Bungay, P.M. and Brenner, H. (1973) The motion of a closely-fitting sphere in a fluid-filled tube. International Journal of Multiphase Flow 1(1), 25-56.

Carballa, M., Omil, F., Lema, J.M., Llompart, M.a., García-Jares, C., Rodríguez, I., Gómez, M. and Ternes, T. (2004) Behavior of pharmaceuticals, cosmetics and hormones in a sewage treatment plant. Water Research 38(12), 2918-2926.

Cath, T.Y., Childress, A.E. and Elimelech, M. (2006) Forward osmosis: Principles, applications, and recent developments. Journal of Membrane Science 281(1-2), 70-87.

Cath, T.Y., Gormly, S., Beaudry, E.G., Flynn, M.T., Adams, V.D. and Childress, A.E. (2005) Membrane contactor processes for wastewater reclamation in space: Part I. Direct osmotic concentration as pretreatment for reverse osmosis. Journal of Membrane Science 257(1-2), 85-98.

Cath, T.Y., Hancock, N.T., Lundin, C.D., Hoppe-Jones, C. and Drewes, J.E. (2010) A multi-barrier osmotic dilution process for simultaneous desalination and purification of impaired water. Journal of Membrane Science 362(1-2), 417-426.

Cornelissen, E.R., Harmsen, D., Beerendonk, E.F., Qin, J.J., Oo, H., de Korte, K.F. and Kappelhof, J.W.M.N. (2011) The innovative Osmotic Membrane Bioreactor (OMBR) for reuse of wastewater. Water Science & Technology 63(8), 1557-1565.

Cornelissen, E.R., Harmsen, D., de Korte, K.F., Ruiken, C.J., Qin, J.-J., Oo, H. and Wessels, L.P. (2008) Membrane fouling and process performance of forward osmosis membranes on activated sludge. Journal of Membrane Science 319(1-2), 158-168.

Cunningham, V.L., Binks, S.P. and Olson, M.J. (2009) Human health risk assessment from the presence of human pharmaceuticals in the aquatic environment. Regulatory Toxicology and Pharmacology 53(1), 39-45.

Elimelech, M. and Phillip, W.A. (2011) The Future of Seawater Desalination: Energy, Technology, and the Environment. Science 333(6043), 712-717.

Gray, G.T., McCutcheon, J.R. and Elimelech, M. (2006) Internal concentration polarization in forward osmosis: role of membrane orientation. Desalination 197(1-3), 1-8.

Hancock, N.T. and Cath, T.Y. (2009) Solute Coupled Diffusion in Osmotically Driven Membrane Processes. Environmental Science & Technology 43(17), 6769-6775.

Hancock, N.T., Xu, P., Heil, D.M., Bellona, C. and Cath, T.Y. (2011) Comprehensive Bench- and Pilot-Scale Investigation of Trace Organic Compounds Rejection by Forward Osmosis. Environmental Science & Technology 45(19), 8483-8490.

Hansen, P.D., Dizer, H., Hock, B., Marx, A., Sherry, J., McMaster, M. and Blaise, C. (1998) Vitellogenin – a biomarker for endocrine disruptors. TrAC Trends in Analytical Chemistry 17(7), 448-451.

Herron, J.R.B., Edward G. Salter, Robert (1997) Direct osmotic concentration contaminated water, OSMOTEK, INC.

Holloway, R.W., Childress, A.E., Dennett, K.E. and Cath, T.Y. (2007) Forward osmosis for concentration of anaerobic digester centrate. Water Research 41(17), 4005-4014.

Israelachvili, J.N. (2010) Intermolecular and Surface Forces, Second Edition: With Applications to Colloidal and Biological Systems, Academic Press.

Lee, S., Boo, C., Elimelech, M. and Hong, S. (2010) Comparison of fouling behavior in forward osmosis (FO) and reverse osmosis (RO). Journal of Membrane Science 365(1-2), 34-39.

López-Muñoz, M.J., Sotto, A., Arsuaga, J.M. and Van der Bruggen, B. (2009) Influence of membrane, solute and solution properties on the retention of phenolic compounds in aqueous solution by nanofiltration membranes. Separation and Purification Technology 66(1), 194-201.

McCutcheon, J.R. and Elimelech, M. (2008) Influence of membrane support layer hydrophobicity on water flux in osmotically driven membrane processes. Journal of Membrane Science 318(1-2), 458-466.

Mi, B. and Elimelech, M. (2008) Chemical and physical aspects of organic fouling of forward osmosis membranes. Journal of Membrane Science 320(1-2), 292-302.

Mi, B. and Elimelech, M. (2010) Organic fouling of forward osmosis membranes: Fouling reversibility and cleaning without chemical reagents. Journal of Membrane Science 348(1-2), 337-345.

Ng, H.Y. and Elimelech, M. (2004) Influence of colloidal fouling on rejection of trace organic contaminants by reverse osmosis. Journal of Membrane Science 244(1-2), 215-226.

Nghiem, L.D. and Coleman, P.J. (2008) NF/RO filtration of the hydrophobic ionogenic compound triclosan: Transport mechanisms and the influence of membrane fouling. Separation and Purification Technology 62(3), 709-716.

Nghiem, L.D., Schäfer, A.I. and Elimelech, M. (2004) Removal of Natural Hormones by Nanofiltration Membranes: Measurement, Modeling, and Mechanisms. Environmental Science & Technology 38(6), 1888-1896.

Nghiem, L.D., Vogel, D. and Khan, S. (2008) Characterising humic acid fouling of nanofiltration membranes using bisphenol A as a molecular indicator. Water Research 42(15), 4049-4058.

Rodgers-Gray, T.P., Jobling, S., Morris, S., Kelly, C., Kirby, S., Janbakhsh, A., Harries, J.E., Waldock, M.J., Sumpter, J.P. and Tyler, C.R. (2000) Long-Term Temporal Changes in the Estrogenic Composition of Treated Sewage Effluent and Its Biological Effects on Fish. Environmental Science & Technology 34(8), 1521-1528.

Schäfer, A.I., Akanyeti, I. and Semião, A.J.C. (2011) Micropollutant sorption to membrane polymers: A review of mechanisms for estrogens. Advances in Colloid and Interface Science 164(1-2), 100-117.

Seidel, A., Waypa, J.J. and Elimelech, M. (2001) Role of Charge (Donnan) Exclusion in Removal of Arsenic from Water by a Negatively Charged Porous Nanofiltration Membrane. Environmental Engineering Science 18(2), 105-113.

Shannon, M.A., Bohn, P.W., Elimelech, M., Georgiadis, J.G., Marinas, B.J. and Mayes, A.M. (2008) Science and technology for water purification in the coming decades. Nature 452(7185), 301-310.

Snyder, S.A., Westerhoff, P., Yoon, Y. and Sedlak, D.L. (2003) Pharmaceuticals, Personal Care Products, and Endocrine Disruptors in Water: Implications for the Water Industry. Environmental Engineering Science 20(5), 449-469.

552 Sutzkover, I., Hasson, D. and Semiat, R. (2000) Simple technique for measuring the
553 concentration polarization level in a reverse osmosis system. Desalination 131(1-3), 117-127.

554 Tang, C.Y., She, Q., Lay, W.C.L., Wang, R. and Fane, A.G. (2010) Coupled effects of
555 internal concentration polarization and fouling on flux behavior of forward osmosis
556 membranes during humic acid filtration. Journal of Membrane Science 354(1-2), 123-133.

557 Tsuru, T., Togoh, M., Wang, X.L., Kimura, S. and Nakao, S. (1995) Evaluation of pore
558 structure and electrical properties of nanofiltration membranes. Journal of chemical
559 engineering of Japan 28(2), 186-192.

560 Valladares Linares, R., Yangali-Quintanilla, V., Li, Z. and Amy, G. (2011) Rejection of
561 micropollutants by clean and fouled forward osmosis membrane. Water Research 45(20),
562 6737-6744.

563 Yangali-Quintanilla, V., Li, Z., Valladares, R., Li, Q. and Amy, G. (2011) Indirect
564 desalination of Red Sea water with forward osmosis and low pressure reverse osmosis for
565 water reuse. Desalination 280(1-3), 160-166.

566 Zou, S., Gu, Y., Xiao, D. and Tang, C.Y. (2011) The role of physical and chemical
567 parameters on forward osmosis membrane fouling during algae separation. Journal of
568 Membrane Science 366(1-2), 356-362.

569

570

571 **Table 1:** Key physicochemical properties of bisphenol A, triclosan, and diclofenac.

Compound		Bisphenol A	Triclosan	Diclofenac
Molecular structure		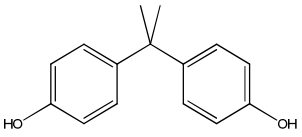	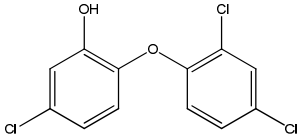	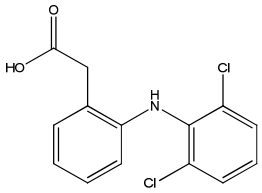
Molecular weight (g/mol)		228.3	289.5	296.2
pK_a [a]		10.3	7.8	4.18
Log D (at pH 7) [a]		3.64	5.28	1.77
Log K_{ow} [a]		3.64	5.34	4.55
Molecular dimension (nm) [b]	Height	0.383	0.693	0.354
	Length	1.068	1.419	0.829
	Width	0.587	0.748	0.700

572 [a] Source: SciFinder Scholar, data calculated using Advanced Chemistry Development (ACD/Labs)

573 Software V8.14 for Scholaris (1994-2007 ACD/Labs)

574 [b] Calculated using Molecular Modelling Pro Version 6.25 (ChemWS)

575 **Table 2**: Estimated mean effective membrane pore radius obtained from reference organic
576 solute experiments

Organic solute	Stokes radius[a] r_s (nm)	$\lambda=r_s/r_p$	Mean effective membrane pore radius r_p (nm)
Erythritol	0.26	0.79	0.33
Xylose	0.29	0.76	0.38
Glucose	0.32	0.80	0.40
Average			0.37

[a] Calculated using the Stokes-Einstein equation

577 **Table 3:** BPA mass adsorption in FO and RO modes (permeate water flux = 5.4 L/m^2·h (1.5
578 µm/s)).

Operating mode	Normalised by membrane area (µg/cm^2)	
	Mass balance calculation	Direct extraction measurement
FO	1.25	1.41
RO	2.07	2.24

579

580 **Table 4:** Triclosan mass adsorption in FO and RO modes (permeate water flux = 5.4 L/m^2·h
581 (1.5 µm/s)).

Operating mode	Normalised by membrane area (µg/cm^2)	
	Mass balance calculation	Direct extraction measurement
FO	4.64	4.42
RO	9.18	8.81

582

583

584 **Table 5:** Diclofenac mass adsorption in FO and RO modes (permeate water flux = 5.4 L/m^2·h
585 (1.5 µm/s)).

Operating mode	Normalised by membrane area (µg/cm^2)	
	Mass balance calculation	Direct extraction measurement
FO	0.196	0.173
RO	0.764	0.422

586 **Table 6**: BPA mass balance in FO (NaCl, $MgSO_4$, and glucose draw solutions) and RO
587 modes (permeate water flux = 5.4 L/m^2·h (1.5 µm/s)).

Operating mode	Draw solution	Reverse solute flux (g/m^2·h)	Normalised by membrane area (µg/cm^2)	
			Mass balance calculation	Direct extraction measurement
FO	NaCl	4.28	1.25	1.41
	$MgSO_4$	0.06	1.98	2.01
	Glucose	0.28	1.82	1.89
RO	Not applicable	0	2.07	2.24

588

589 LIST OF FIGURES

590 **Figure 1:** BPA concentration in feed and permeate and rejection as a function of time in the
591 (a) FO mode and (b) RO mode at the same permeate water flux of 5.4 L/m^2·h (1.5 µm/s). The
592 FO experimental conditions were as follows: the initial concentrations of BPA in the feed =
593 500 µg/L, pH = 7, the background electrolyte contained 20 mM NaCl and 1 mM $NaHCO_3$,
594 draw solution = 0.5 M NaCl, cross flow rate = 1 L/min for both sides, and cross flow velocity
595 = 9 cm/s. The temperature = 25±1 °C for both sides. The error bars represent standard
596 deviation of data obtained from two independent experiments. The RO experimental
597 conditions were as follows: the initial concentrations of BPA in the feed = 500 µg/L, pH = 7,
598 the background electrolyte contained 20 mM NaCl and 1 mM $NaHCO_3$. Operating pressure
599 10 bar, cross flow rate = 1 L/min, cross flow velocity = 25 cm/s, temperature = 25±1 °C.

600 **Figure 2:** Triclosan concentration in feed and permeate and rejection as a function of time in
601 (a) FO mode and (b) RO mode. The initial concentration of triclosan in the feed = 500 µg/L
602 both in the FO and RO experiments. Other experimental conditions were described in Figure
603 1.

604 **Figure 3:** Diclofenac concentration in feed and permeate and rejection as a function of time
605 in (a) FO mode and (b) RO mode. The initial concentration of diclofenac in the feed = 500
606 µg/L both in the FO and RO experiments. Other experimental conditions were described in
607 Figure 1.

608 **Figure 4:** Schematic diagram representing the retarded forward diffusion of feed solutes in
609 the FO process by the reverse draw solutes.

610 **Figure 5:** BPA concentration in feed and permeate and rejection as a function of time in the
611 FO mode using approximately (a) 3 M glucose and (b) 2.5 M $MgSO_4$ as draw solution. The
612 permeate water flux was 5.4 L/m^2·h (1.5 µm/s). Other FO experimental conditions were as
613 described in Figure 1.

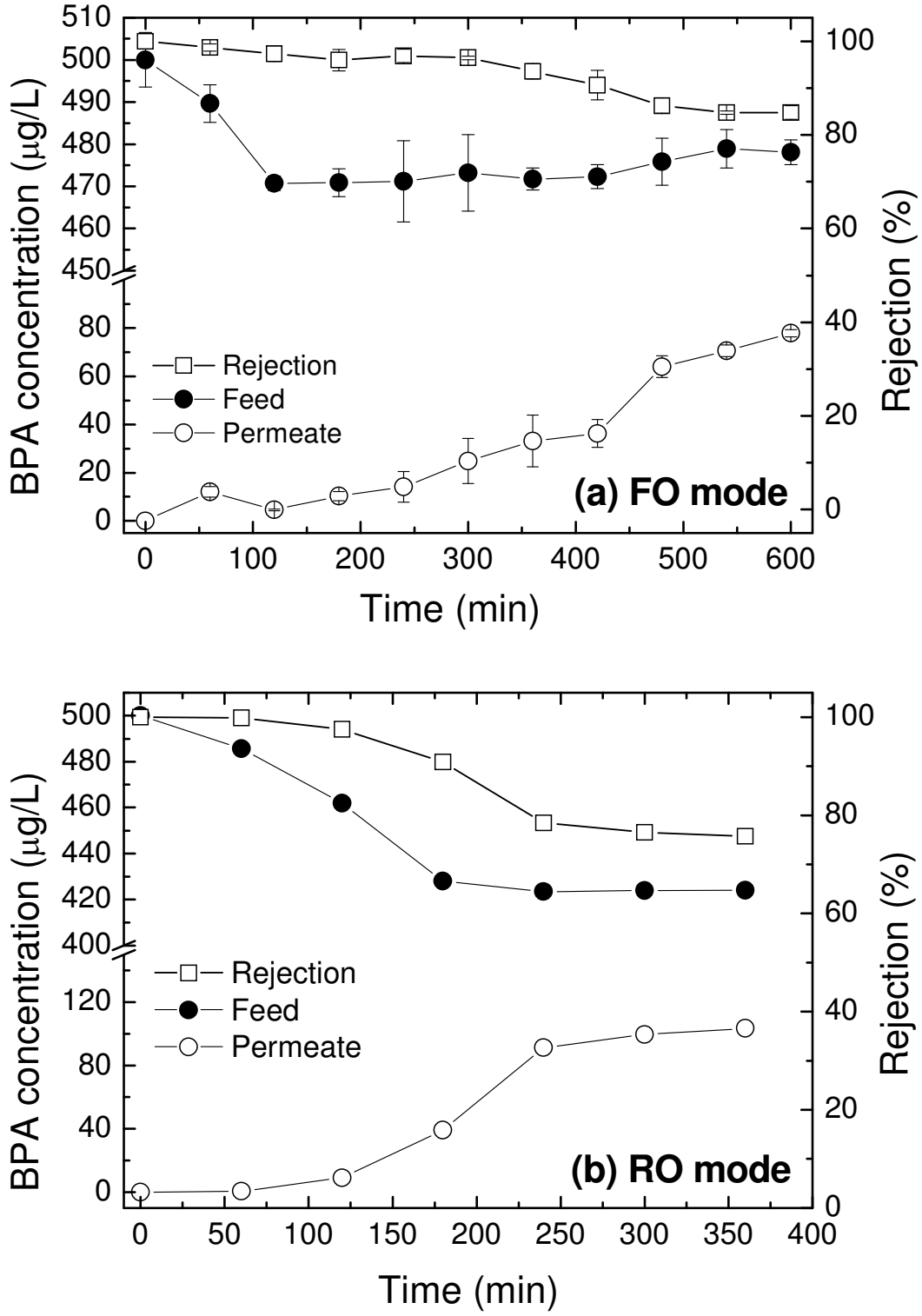

614

615 **Figure 1**

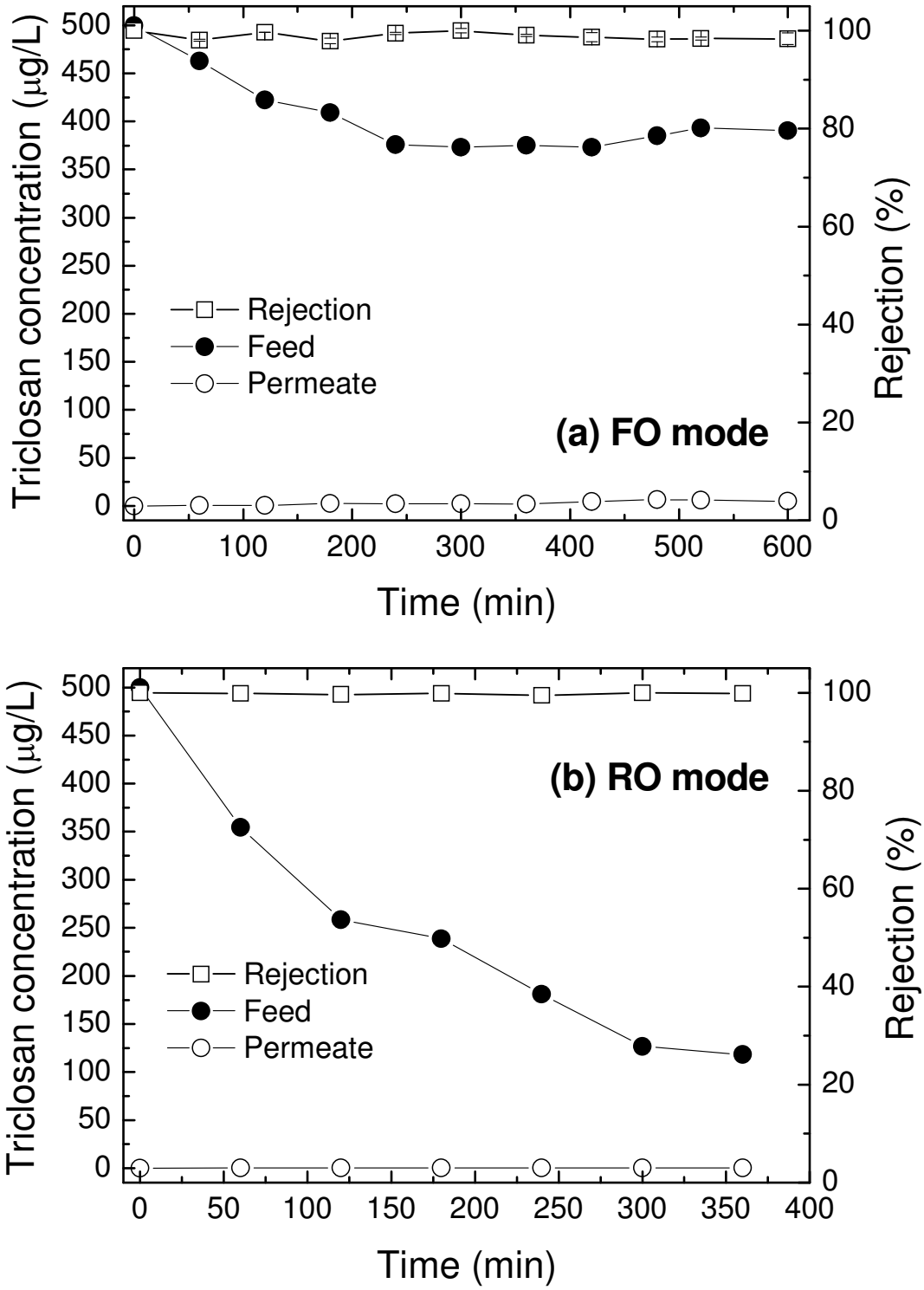

616

617 **Figure 2**

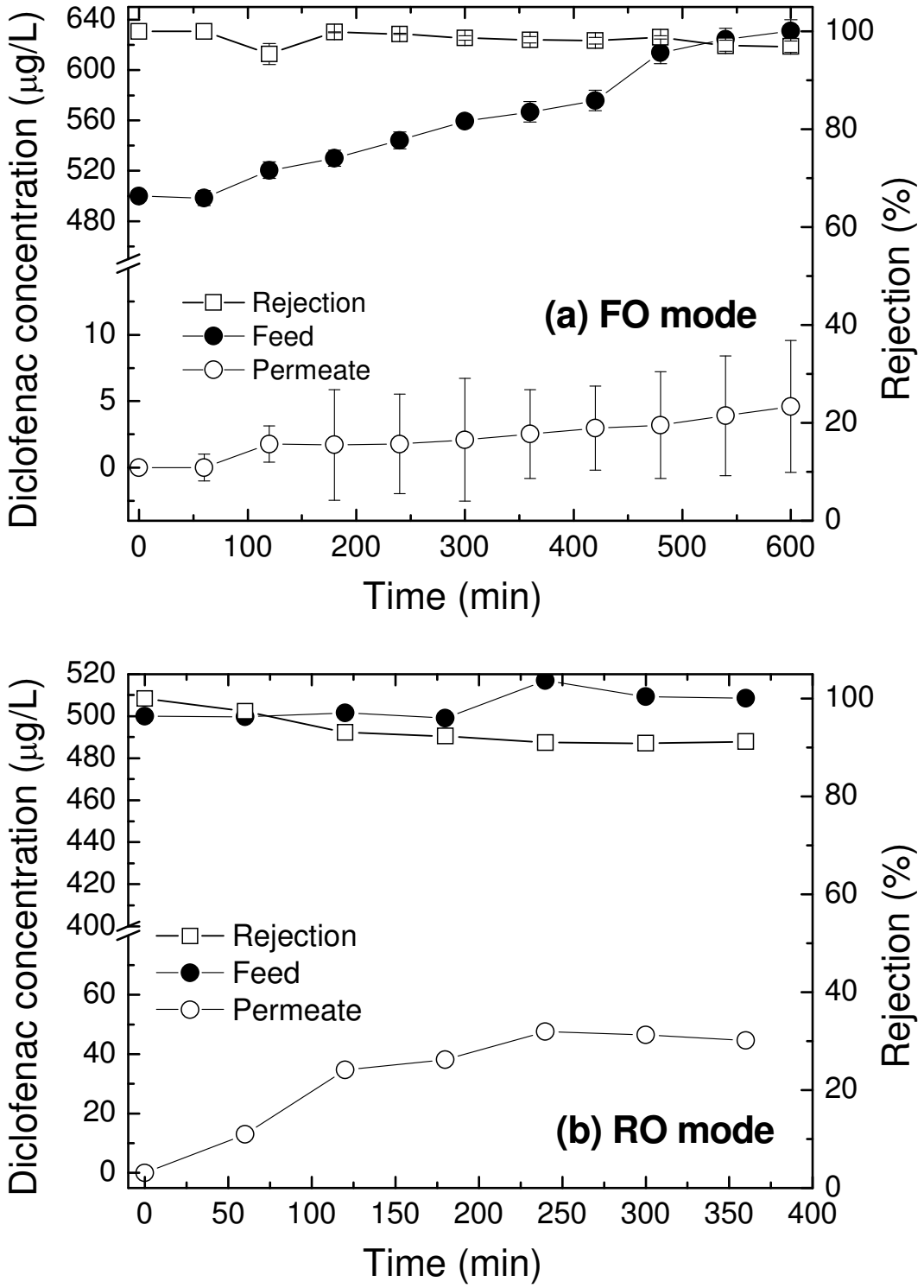

618

619 **Figure 3**

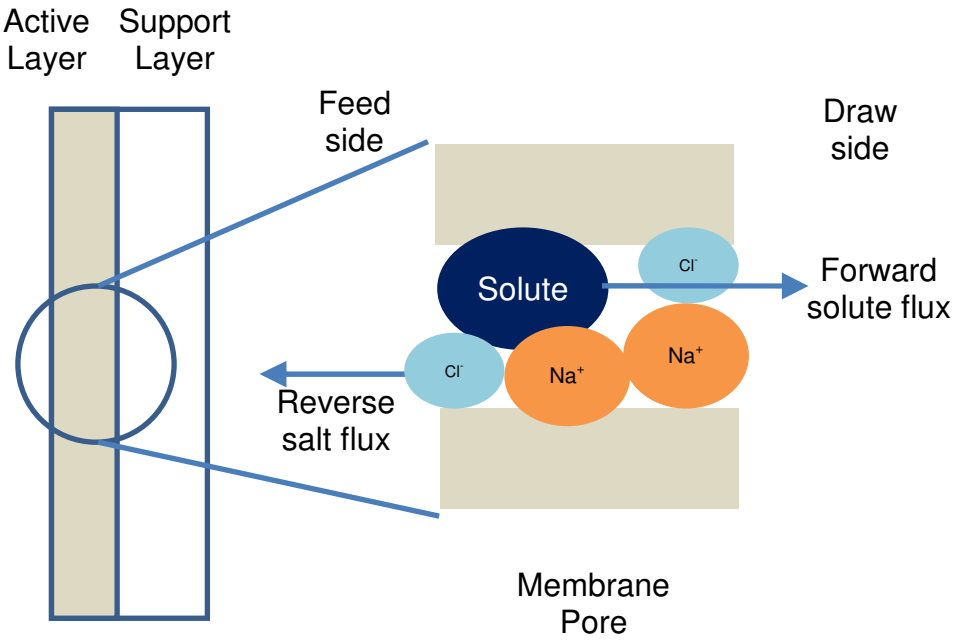
Active Layer
Support Layer
Feed side
Draw side
Solute
Cl-
Forward solute flux
Cl-
Na+
Na+
Reverse salt flux
Membrane Pore

Figure 4

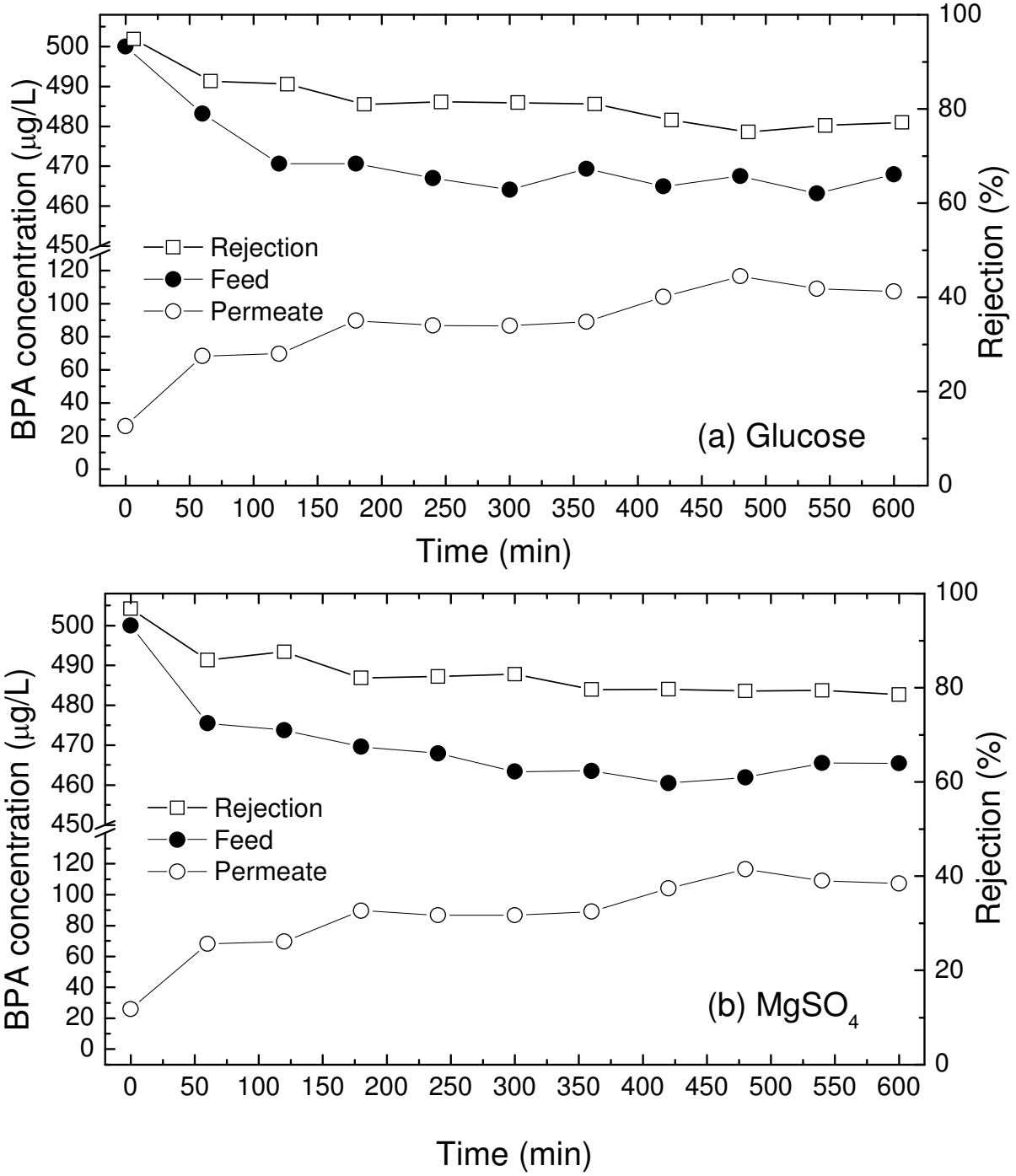

639
640 **Figure 5**